

A Photogrammetric Method for Spatial Data Extraction from Google Earth and Improvement with Precision Analysis

Sadegh Karimi ^a, Ehsan Khorrambakht ^{b*}

^a Department of Geomatics Engineering, K. N. Toosi University of Technology, Tehran, Iran.

^b Department of Aerospace Engineering, K. N. Toosi University of Technology, Tehran, Iran.

Received 05 January 2018; Accepted 17 April 2018

Abstract

Topography maps are crucial for civil engineering projects, such as road construction, water channel construction, urban construction, and mining. Here we present a method which enables us to extract topographical map via modeling Google Earth and some field works. In this method, first, we model Google Earth as an object with closed-range photogrammetric method in the Agisoft Photoscan. Through some field works, we measured twenty-two points including twelve ground control points (GCP) and ten independent check points (ICP). Due to these GCPs, we were able to transform our model to real world with global polynomial and multi-quadratic equations and ICPs were used for precision analysis. This method is easy and cheap to obtain spatial data and the accuracy is sufficient for research requirements.

Keywords: Photogrammetric Method; Data Extraction; Google Earth; Modelling; Agisoft Photoscan; Data Processing; Multi-quadratic Transformation.

1. Introduction

Google Earth is used widely among researchers as a virtual globe which provides many free satellite images and three-dimensional views of Earth [1]. The most prevalent use of Google Earth by researchers is to put their own collected data on the background images and observe the geographical context [2]. The use of Google Earth is classified into some main objectives, namely visualization, data collecting, data exploration, data integration, modelling and simulation, validation and decision support by Goodchild and Stensgaard [3-4]. The quality of images varies from place to place and the accuracy may not be suitable for some research purposes at certain locations in which case image processing is necessary for accurate data collection [5-8]. Use of single coordinate system which is WGS84, easy visualization and accessible data, and freely accessible remotely sensed images are the advantages of Google Earth, but the inconsistency in the accuracy of its data is one of its disadvantages [1]. A way to solve this problem is to integrate a database collected during field works and the data produced by the digital map which needs some further processing [9] and conversions [2, 10].

In this article, a novel method is presented to extract data from google earth with higher accuracy. First, Google-Earth is remodeled using a photogrammetric method. Furthermore, transformation from model coordinate system to ground coordinate system is done by global polynomial and multi-quadric equations. Finally, the topography of a region is created in UTM coordinate system. The flowchart of research is shown in Figure 1.

* Corresponding author: ekhorrambakht@email.kntu.ac.ir

 <http://dx.doi.org/10.28991/cej-0309141>

➤ This is an open access article under the CC-BY license (<https://creativecommons.org/licenses/by/4.0/>).

© Authors retain all copyrights.

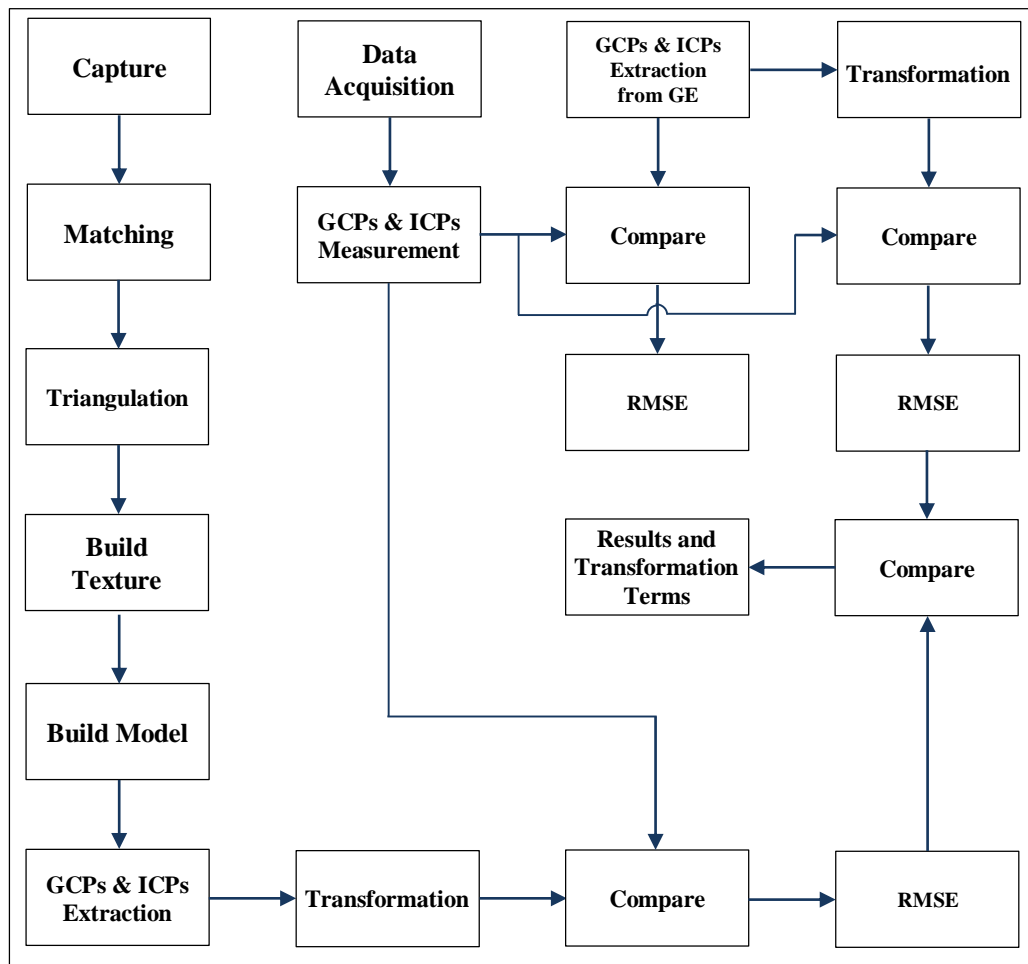


Figure 1. Research Flowchart

2. Methodology

2.1. Structure

Google Earth is a free source of spatial data which has many users. Accuracy of Google Earth is different in various regions. One of its features is presenting a good visual space. Google Earth gives us an option to capture images with different resolution. Our images were taken with 4800×2718 resolution. Several images were taken from various views which overlap with each other like as modeling an object in closed-range photogrammetry.

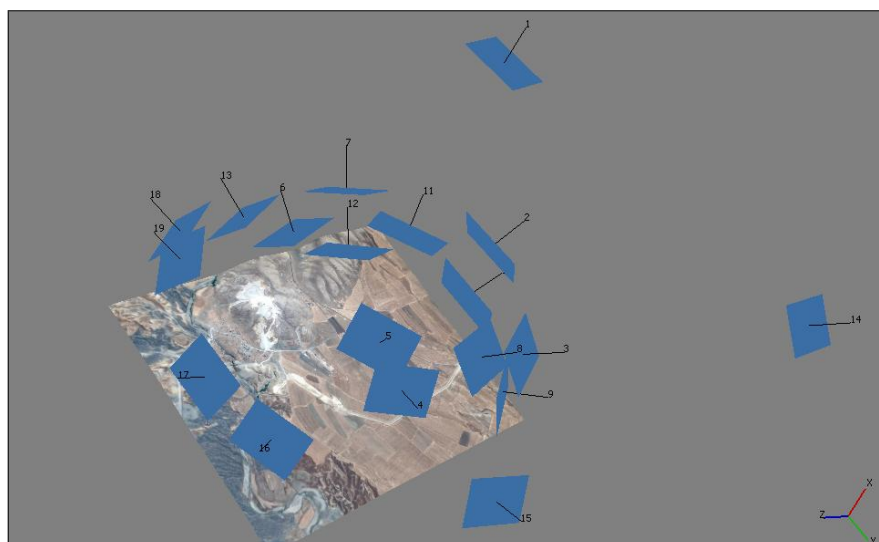


Figure 2. Capturing the area form various views

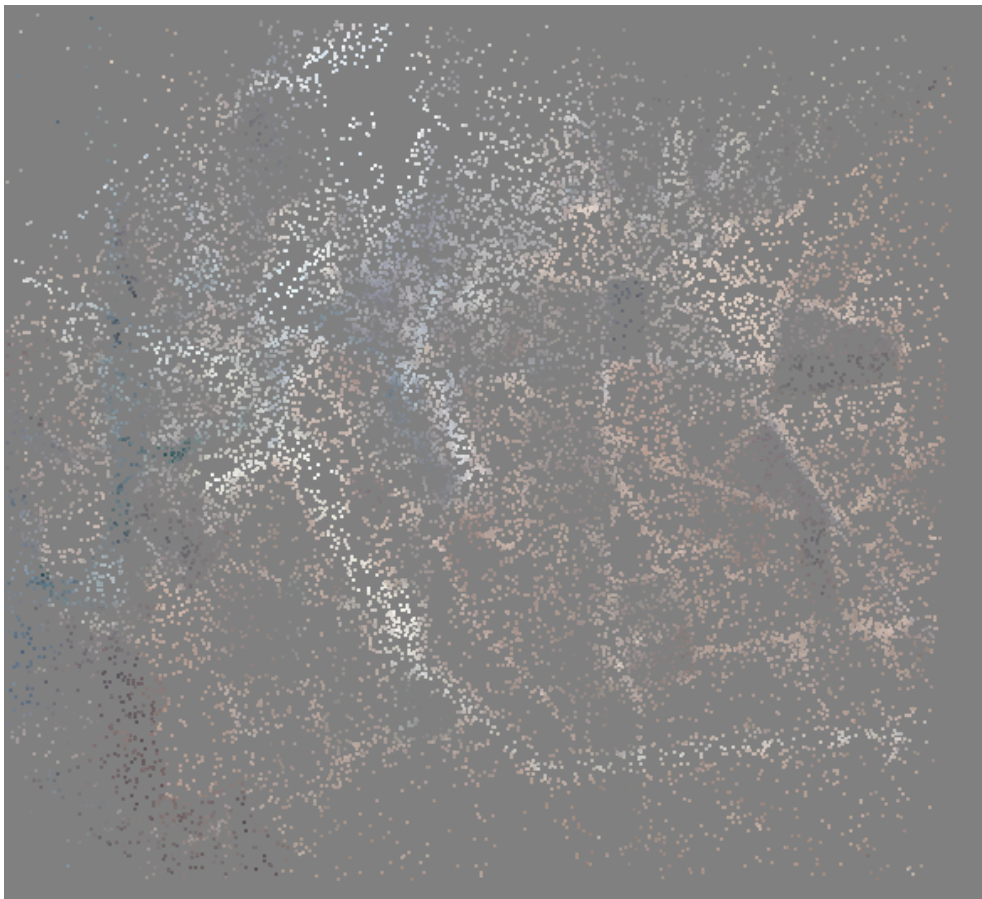
In order to image processing to build the model, several photogrammetric processing software exist. These include Australis, Photomod, PhotoModeler and Agisoft Photoscan. Since Agisoft Photoscan is a low cost software and also has high capabilities, we used it for our image processing purposes.

Agisoft Photoscan is able to detect conjugate points by performing automatic matching. The workflow of the software is presented as follow: after adding images to workspace, photos are aligned and corresponding points are determined; then dense cloud is constructed and depth filtering is applied; after that the discrete space is interpolated into a continuous space and a triangular mesh is built which forms a DSM; finally, a texture is built based on orthophoto mapping mode and mosaic blending mode. Although the algorithm used in Agisoft Photoscan is inaccessible, we are able to assume that it is based on bundle adjustment since adjustment of all images is done simultaneously in a single block of photogrammetry which means all the rays that go through the principle center of images are simultaneously adjusted. Basis of mathematical models for bundle block adjustment is the collinearity equation, given below:

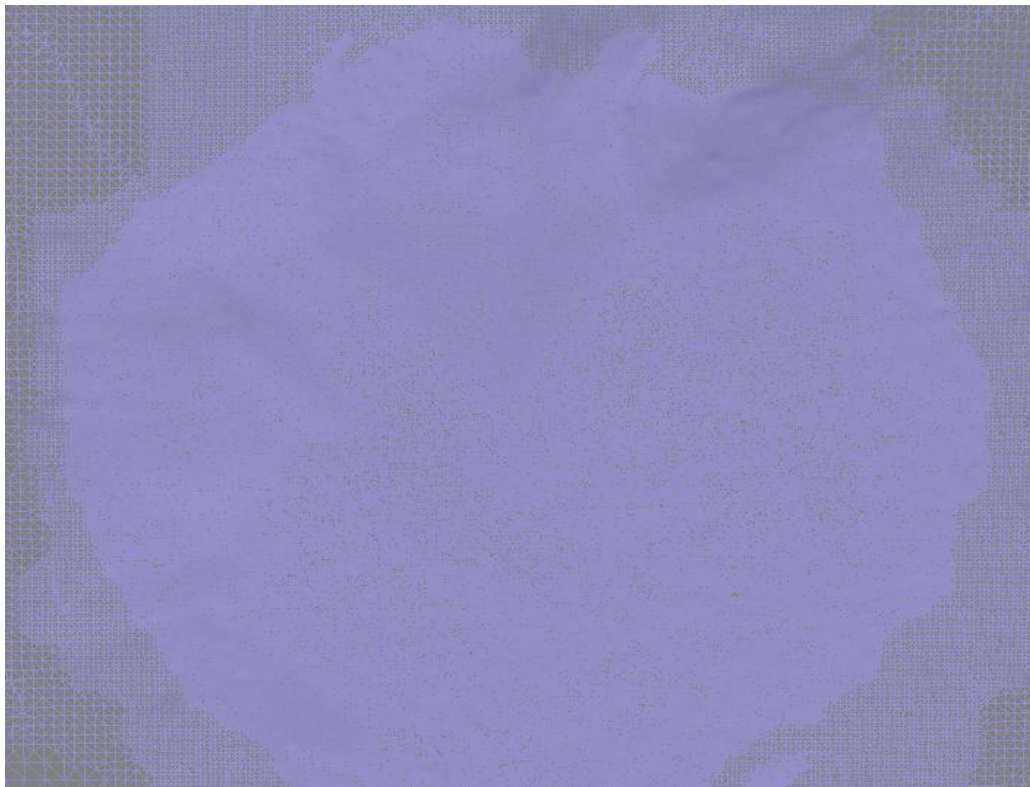
$$\vec{r} = K \cdot M_{\omega\phi\kappa} \cdot \vec{R}$$

$$\begin{bmatrix} x - x_0 \\ y - y_0 \\ -c \end{bmatrix} = K \cdot M_{\omega\phi\kappa} \cdot \begin{bmatrix} X - X_0 \\ Y - Y_0 \\ Z - Z_0 \end{bmatrix} \quad (1)$$

Where x, y are coordinates of image points stated in photogrammetry imagery coordination system; $x_0, y_0, -c$ are interior orientation parameters; $X_0, Y_0, Z_0, \omega, \phi, \kappa$ are exterior orientation parameters; X, Y, Z are coordinates of ground points stated in ground coordination system, but GCPs are not used in the model space generated by Agisoft Photoscan and the transformation of model's arbitrary coordination system to ground coordination system is done by global polynomial and multi-quadric equations.



(a)



(b)



(c)

Figure 3. (a) Point Cloud, (b) Triangulation, (c) Assign texture to DSM

The coordination system for our model is chosen arbitrary. The positional and elevation data of GCPs and ICPs are exported due to this coordination system. After model is built, we can export points, orthophoto, DEM, and also interior orientation parameters of camera. Since we didn't use a camera, interior orientation parameters were assumed free (self-

calibration) in our equations. The interior orientation parameters of camera are as follow: C is the focal length; X_p, Y_p are principal point coordinates; K_1, K_2, K_3 are radial distortion polynomial coefficients; P_1, P_2 are tangential distortion coefficients.

2.2. Field Work (Data Acquisition)

The considered region is placed in Iran, Kermanshah with $34^{\circ}47.85' - 34^{\circ}45.1'N$ and $45^{\circ}50.05' - 45^{\circ}51.3'E$. This region is slightly more than $3km^2$. Figure 4 shows the location of the study. GCPs and ICPs are shown with red and yellow markers, respectively.

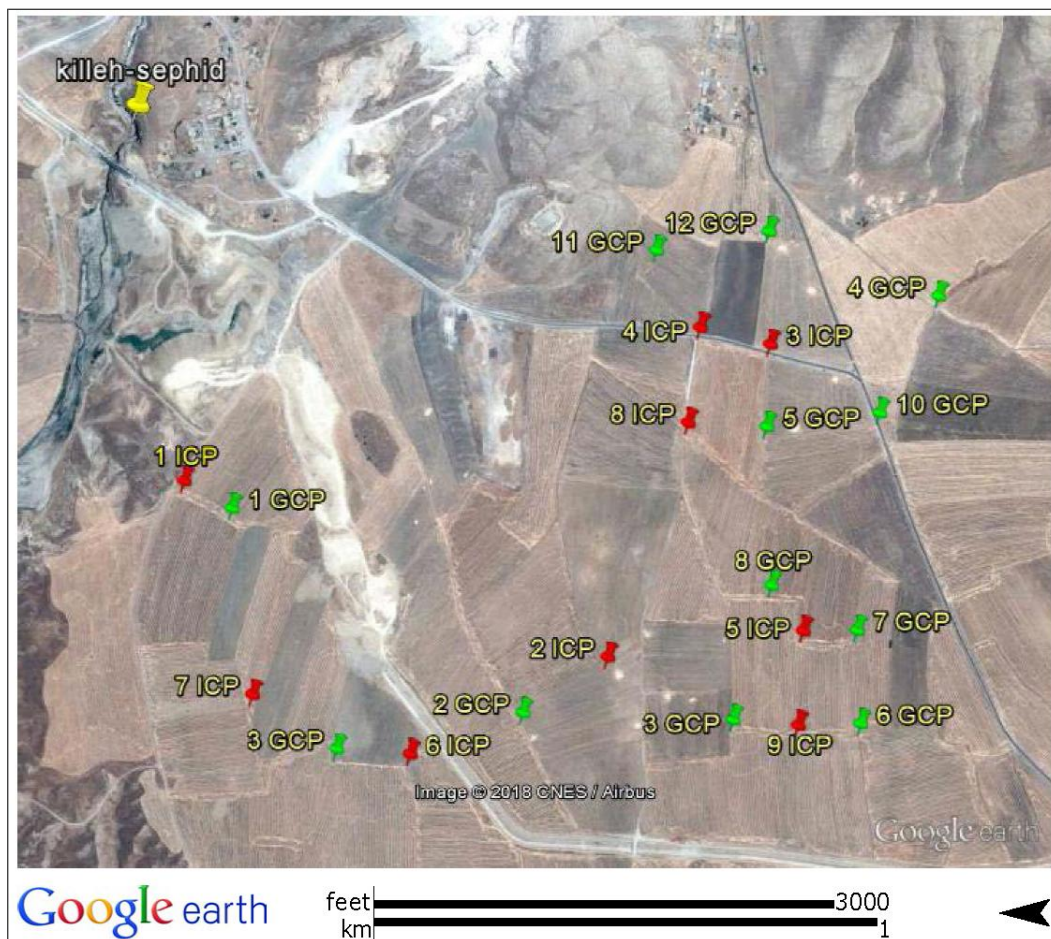


Figure 4. The location of GCPs and ICPs in the studied region

The coordination of benchmark points was determined in Universal Transverse Mercator (UTM) coordinate system by dual frequency GPS. Benchmark points are used in order to enable total station to determine the coordinate system. The total station used is Leica TS09 and the coordinates of GCPs and ICPs were measured by it. The points are shown in Figure 3.

Table 1. Measured coordinate of points by dual frequency GPS

Point	X (m)	Y (m)	Z (m)
1 ICP	577287.255	3845314.205	599.777
2 ICP	576942.437	3844475.296	597.794
3 ICP	577562.921	3844161.106	607.281
4 ICP	577595.499	3844298.241	606.808
5 ICP	576996.776	3844091.762	598.51
6 ICP	576746.384	3844864.676	591.369
7 ICP	576864.79	3845175.076	597.291
8 ICP	577407.832	3844320.858	604.353
9 ICP	576808.866	3844099.519	593.936
1 GCP	577233.93	3845218.583	599.248

2 GCP	576830.802	3844642.699	595.697
3 GCP	576756.078	3845009.054	591.709
4 GCP	576818.644	3844227.388	595.369
5 GCP	577656.709	3843839.39	619.443
6 GCP	577400.797	3844166.419	605.488
7 GCP	576812.355	3843976.87	596.652
8 GCP	576998.891	3843985.973	600.154
9 GCP	577086.448	3844154.229	599.456
10 GCP	577428.406	3843946.88	609.604
11 GCP	577745.917	3844385.761	612.68
12 GCP	577783.926	3844166.632	610.806

Table 2. Coordinate of points observed from Google-Earth

Point	X (m)	Y (m)	Z (m)
1 ICP	577273.04	3845320.98	595
2 ICP	576917.2	3844474.09	596
3 ICP	577537.43	3844160.22	606
4 ICP	577577.8	3844293.73	606
5 ICP	576969.88	3844091.43	598
6 ICP	576722.23	3844866.55	591
7 ICP	576842.44	3845172.32	595
8 ICP	577382.55	3844323.12	602
9 ICP	576781.78	3844096.34	593
1 GCP	577214.06	3845217.56	598
2 GCP	576806.11	3844638.09	594
3 GCP	576733.32	3845006.11	590
4 GCP	576796.33	3844225.34	593
5 GCP	577628.98	3843843.21	619
6 GCP	577375.91	3844166.19	603
7 GCP	576789.04	3843972.06	594
8 GCP	576972.45	3843981.83	598
9 GCP	577058.34	3844157.65	598
10 GCP	577400.24	3843946.78	608
11 GCP	577719.3	3844386.09	612
12 GCP	577756.45	3844164.62	612

Table 3. Difference between measured and observed coordinate of points

Point	dX (m)	dY (m)	dZ (m)
1 ICP	14.215	-6.775	4.777
2 ICP	25.237	1.206	1.794
3 ICP	25.491	0.886	1.281
4 ICP	17.699	4.511	0.808
5 ICP	26.896	0.332	0.51
6 ICP	24.154	-1.874	0.369
7 ICP	22.35	2.756	2.291
8 ICP	25.282	-2.262	2.353
9 ICP	27.086	3.179	0.936
1 GCP	19.87	1.023	1.248
2 GCP	24.692	4.609	1.697

3 GCP	22.758	2.944	1.709
4 GCP	22.314	2.048	2.369
5 GCP	27.729	-3.82	0.443
6 GCP	24.887	0.229	2.488
7 GCP	23.315	4.81	2.652
8 GCP	26.441	4.143	2.154
9 GCP	28.108	-3.421	1.456
10 GCP	28.166	0.1	1.604
11 GCP	26.617	-0.329	0.68
12 GCP	27.476	2.012	-1.194
RMSE	25.3773 (m)		1.9748

The measured GCPs and ICPs are compared with Google-Earth software, and the corresponding root mean square is computed (Table 3). Due to the similar shifts to east in the points and the great value of RMSE, a systematic error exists. In order to resolve these errors, Global Polynomial and Multi-Quadric transformations will be used in next section.

2.3. Transformations

2.3.1. Global Polynomial and Multi-Quadric Equations

In the presented method, mathematical statistics equations are used to transform Google Earth and our model to real world, in which we measured GCPs and ICPS. Global polynomial is a completely interpolative statistic equation that is used up to third order (cubic terms) for the transformation. The following equations represent third order Global Polynomial:

$$\begin{aligned}
 X &= a_0 + a_1x + a_2y + a_3xy + a_4x^2 + a_5y^2 + a_6xy^2 + a_7x^2y + a_8x^3 + a_9y^3 \\
 Y &= b_0 + b_1x + b_2y + b_3xy + b_4x^2 + b_5y^2 + b_6xy^2 + b_7x^2y + b_8x^3 + b_9y^3 \\
 H &= c_0 + c_1h + c_2h^2 + c_3
 \end{aligned}
 \tag{2}$$

Where X, Y, H are the transformed coordinates (GCPs and ICPs coordinates); x, y, h are the coordinates of Google-Earth or model which should be transformed; $\{a_i, b_i, c_i, i = 0, \dots, k\}$ are the coefficients calculated by GCPs. Note that (a_i, b_i) is a pair of terms for positional transformation and c_i is a single term for height transformation.

Generally, multi-quadric equations are developed form of point-wise equations. The amount of refinement and correction of these equations depends on different parameters of ground control points such as distribution, quantity and accuracy. After applying global polynomial, a deviation for X, Y, H could be calculated (dX, dY, dH) and used in the following equations (multi-quadric equations):

$$\begin{aligned}
 dX_i &= \sum_{j=1}^n \alpha_j F_{ji} = \alpha_1 F_{1i} + \alpha_2 F_{2i} + \dots + \alpha_n F_{ni} \\
 dY_i &= \sum_{j=1}^n \beta_j F_{ji} = \beta_1 F_{1i} + \beta_2 F_{2i} + \dots + \beta_n F_{ni} \\
 dH_i &= \sum_{j=1}^n \gamma_j G_{ji} = \gamma_1 G_{1i} + \gamma_2 G_{2i} + \dots + \gamma_n G_{ni}
 \end{aligned}
 \tag{3}$$

where $\alpha_j, \beta_j, \gamma_j$ are coefficients; F_{ji} is the distance from j th control point to the i th control point in the horizontal plane; G_{ji} is height difference of j th and i th control point. Therefore we could easily deduce that $F_{ii} = 0, F_{ij} = F_{ji}, G_{ii} = 0, G_{ij} = G_{ji}$. From the above equations we are able to calculate the coefficients $\{\alpha_j, \beta_j, \gamma_j\}$. Then the deviation of unknown points could be calculated as follow:

$$dX_U = \sum_{j=1}^n \alpha_j F_j = \alpha_1 F_1 + \alpha_2 F_2 + \dots + \alpha_n F_n
 \tag{4}$$

$$dY_U = \sum_{j=1}^n \beta_j F_j = \beta_1 F_1 + \beta_2 F_2 + \dots + \beta_n F_n$$

$$dH_U = \sum_{j=1}^n \gamma_j G_j = \gamma_1 G_1 + \gamma_2 G_2 + \dots + \gamma_n G_n$$

Where F_j is the distance between an unknown point and the i th control point in the horizontal plane; G_j is the height difference of an unknown point from the i th control point. Finally, the unknown point coordination is calculated:

$$(X, Y, H)_{unknown\ point}^{final\ multi-quadric} = (X, Y, H)_{unknown\ point}^{global\ polynomial} + (dX, dY, dH)_U \tag{5}$$

2.3.2. Accuracy Assessment

In this section we will use ICPs to check the accuracy of the calculations. As we know, ICPs are dealt with like unknown points. By using GCPs, we derive the distance between GCPs and ICPs as follows:

$$(X, Y, H)_{ICP}^{final\ multi-quadric} = (X, Y, H)_{ICP}^{global\ polynomial} + (dX, dY, dH)_{ICP} \tag{6}$$

$$(dX, dY, dH)_{ICP}^{multi-quadric} = (X, Y, H)_{ICP}^{measured} - (X, Y, H)_{ICP}^{final\ multi-quadric} \tag{7}$$

$$RMSE_{ICP}^{multi-quadric} = \sqrt{\frac{\sum_{i=1}^n dr_i^2}{n - 1}} \tag{8}$$

Where $dr_i = \sqrt{dX_i^2 + dY_i^2}$ for positional, and $dr_i = dH_i$ for height.

3. Results and Discussion

One of the outputs of Agisoft which was orthophoto has many applications as a photogrammetry output. This output could be used as data for remote sensing softwares such as ENVI, after being georeferenced. RS analysis results in cadastral mapping, vegetation maps and watershed mapping. Also it could lead to change detection of a region if orthophoto of different dates exists, and using Google Earth which contains dated photos in the presented method will make it possible. Figure 5 shows the orthophoto of modelled region.



Figure 5. Orthophoto of the region modeled in Agisoft Photoscan

In our measurements, we had an elevation control point named “Killeh Sefhid Valley”. This control point was not considered due to the high difference of its measured value (556.43 m) and its value in Google Earth (590 m). Therefore, error of Google Earth in this point is high since it couldn’t calculate the depth of Killeh Sefhid Valley.

Table 4 and 5 respectively, show the height and horizontal RMSE for global polynomial and multi-quadric transformations. Various polynomials have been checked and among them the best transformation which has the minimum RMSE are highlighted.

Table 4. Height RMSE comparison between Google-Earth and model, with different transformations

No. of Terms	Google Earth Height RMSE				Model Height RMSE			
	Global Polynomial		Multi-Quadric		Global Polynomial		Multi-Quadric	
	GCP	ICP	GCP	ICP	GCP	ICP	GCP	ICP
1	8.5	6.18	0	0.15	8.47	6.56	0	0.14
2	0.51	1.38	0	1.34	0.78	1.4	0	1.31
3	0.47	1.35	0	1.4	0.77	1.36	0	1.35
4	0.47	1.34	0	1.41	0.71	1.3	0	1.4
5	0.47	1.34	0	1.41	0.71	1.3	0	1.4
6	0.47	1.34	0	1.41	0.71	1.3	0	1.41
7	0.47	1.34	0	1.41	0.71	1.3	0	1.41
8	0.47	1.34	0	1.41	0.71	1.3	0	1.41

According to Table 4, the most effective transformation in order to reduce RMSE is zero-order Multi-Quadric. RMSE of the transformed model and the measured values is 14 cm.

Table 5. Horizontal RMSE comparison between Google-Earth and model, with different transformations

Pairs of Terms	Google Earth Horizontal RMSE				Model Horizontal RMSE			
	Global Polynomial		Multi-Quadric		Global Polynomial		Multi-Quadric	
	GCP	ICP	GCP	ICP	GCP	ICP	GCP	ICP
3	2.8187	4.4857	0	4.4961	3.3055	6.1948	0	6.157
4	2.8186	4.4857	0	4.4961	3.2057	6.2981	0	6.1454
5	2.6994	4.6984	0	4.5627	2.6841	6.5035	0	6.3664
6	2.738	4.6688	0	4.5423	2.3747	6.9608	0	6.5713
7	2.8791	4.7725	0	4.5503	2.3691	7.0189	0	6.5972
8	2.7688	4.7684	0	4.5686	2.2293	7.1586	0	6.6675
9	2.4826	4.4365	0	4.6019	1.8089	5.5118	0	5.3837
10	2.653	4.8342	0	4.6789	1.3863	5.6305	0	5.4725

Figure 6 and 7 are respectively, plots of elevation and horizontal RMSE for ICPs with multi-quadric transformation. As it’s obvious in Figure 6, error of the model is approximately equal to the error of Google-Earth. As it is seen in Figure 7, the best transformation to reduce horizontal RMSE is multi-quadric method with 9 pairs of terms. Model transformation with this method reduces the error with respect to measured values to 5.38 (m). The difference of this method with respect to Google-Earth is less than 1 meters.

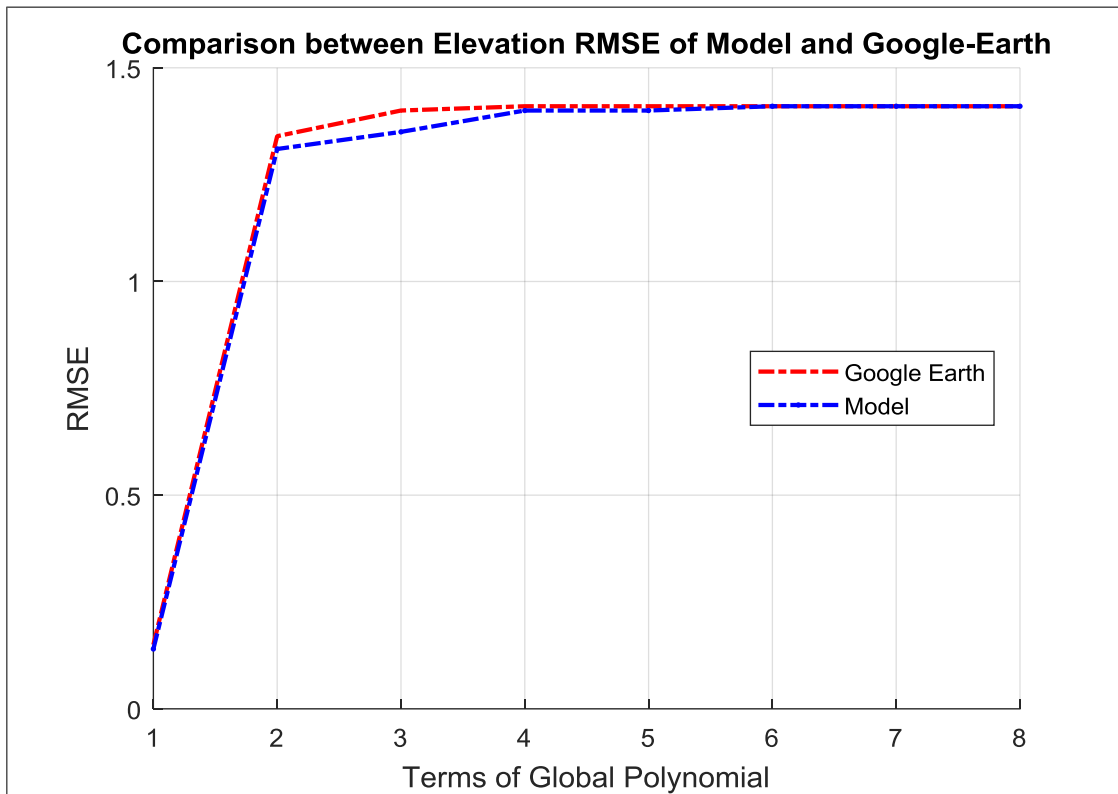


Figure 6. Comparison between Elevation RMSE of Model and Google-Earth

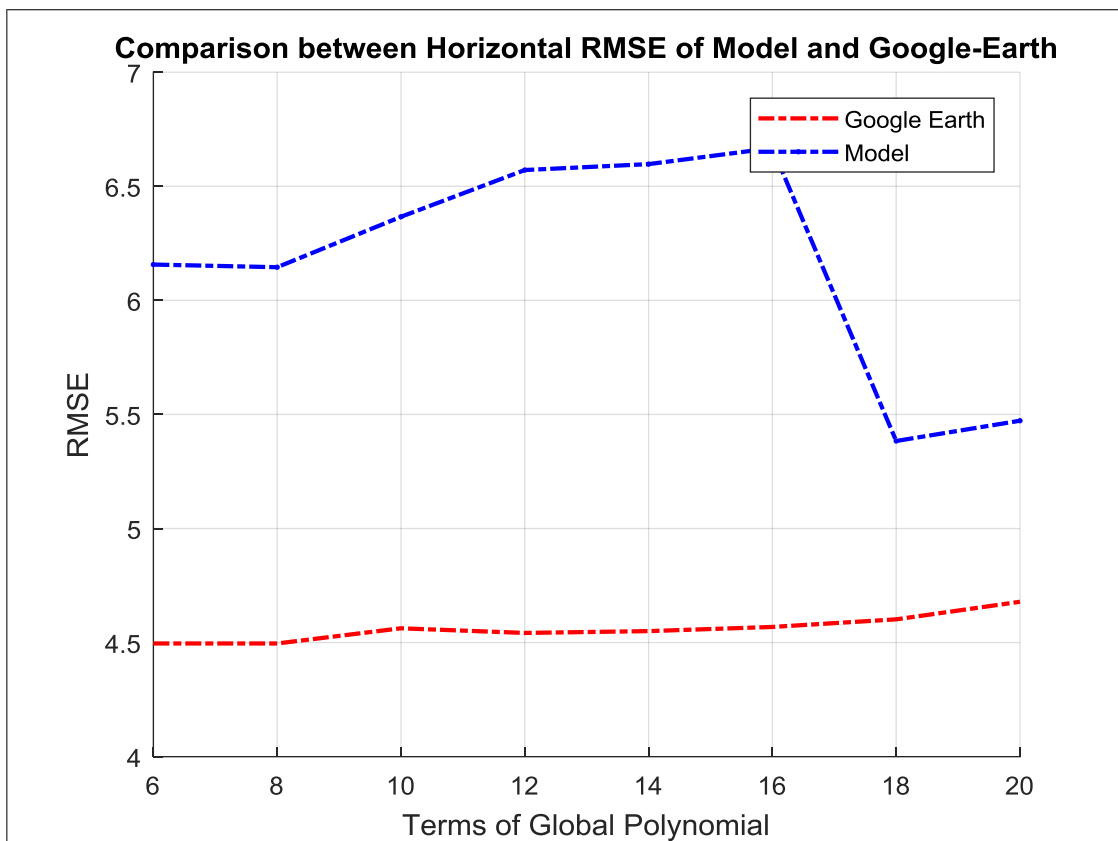


Figure 7. Comparison between Horizontal RMSE of Model and Google-Earth

One of the outputs of Agisoft is generated DTM. Points exported from this DTM are transformed with the ideal transformation equation, and then used to create the georeferenced topography of the region in UTM coordinate system.

4. Conclusion

The method presented in this study could model the topology of a region with 5.3837 RMSE in horizontal and 0.14 RMSE in elevation. Since it was based on photogrammetric modeling of Google-Earth, the costs were low but the errors of Google-Earth affected our results. However, adding images from UAV or other satellite would improve the accuracy of the method.

From other advantages of this method we could mention being more supervised than Civil 3d and SketchUp where contours are automatically transferred from Google Earth to software. Also the accuracy is acceptable for studies and civil engineering projects with this much accuracy requirements. Places where have been changed due to natural/human causes and primary topography data is not available, our topography is the only reference which could be used as primary topography.

We encountered several challenges during this study. First of all, GCPs and ICPs were selected on the corner of the borders of farms, which its width about 40cm, adds approximately 20cm horizontal error in our work. Another challenge was destruction of borders due to human actions in the middle of the studied region where we weren't able to select any ground control points. We couldn't use Google-Earth data for Killeh Sefhid Valley ground control point due to its high errors; Taking images with UAV from this valley and adding the model created by them to our model will make us able not only to improve our model but also presents a correction for Google-Earth.

5. References

- [1] L. Yu and P. Gong, "Google Earth as a virtual globe tool for Earth science applications at the global scale: progress and perspectives," *International Journal of Remote Sensing* (December 2011): 3966–3986. doi: 10.1080/01431161.2011.636081.
- [2] N. H. Oberlies, J. I. Rineer, F. Q. Alali, K. Tawaha, J. O. Falkinham, and W. D. Wheaton, "Mapping of sample collection data: GIS tools for the natural product researcher," *Phytochemistry Letters* (February 2009): 1–9. doi: 10.1016/j.phytol.2008.10.006.
- [3] M. F. Goodchild, "The use cases of digital earth," *International Journal of Digital Earth* (March 2008): 31–42. doi: 10.1080/17538940701782528.
- [4] A.-S. Stensgaard, C. F. L. Saarnak, J. Utzinger, P. Vounatsou, C. Simoonga, G. Mushingi, C. Rahbek, F. Møhlenberg, and T. K. Kristensen, "Virtual globes and geospatial health: the potential of new tools in the management and control of vector-borne diseases," *Geospatial health* (May 2009): 127. doi: 10.4081/gh.2009.216.
- [5] S. Bernabé and A. Plaza, "A new system to perform unsupervised and supervised classification of satellite images from Google Maps," *Satellite Data Compression, Communications, and Processing VI* (August 2010). doi: 10.1117/12.863243.
- [6] P. Gong, Z. Li, H. Huang, G. Sun, and L. Wang, "ICESat GLAS Data for Urban Environment Monitoring," *IEEE Transactions on Geoscience and Remote Sensing* (March 2011): 1158–1172. doi: 10.1109/tgrs.2010.2070514.
- [7] J. Guo, P. Gong, and L. Liang, "Removing shadows from Google Earth satellite images," *Geoinformatics 2007: Remotely Sensed Data and Information* (June 2007). doi: 10.1117/12.760102.
- [8] C. Mering, J. Baro, and E. Upegui, "Retrieving urban areas on Google Earth images: application to towns of West Africa," *International Journal of Remote Sensing* (December 2010): 5867–5877. doi: 10.1080/01431161.2010.512311.
- [9] A. Chen, G. Leptoukh, S. Kempler, D. Nadeau, and X. Zhang, "Augmenting the Research Value of Geospatial Data using Google Earth," *Journal of the Virtual Explorer* (2008). doi: 10.3809/jvirtex.2008.00194.
- [10] Y. Yamagishi, K. Suzuki, H. Tamura, H. Nagao, H. Yanaka, and S. Tsuboi, "Integration of geophysical and geochemical data," *AGU Fall Meeting Abstracts* (December 2006).
- [11] <https://earth.google.com/web/>.